

**DESIGN AND FABRICATION OF A WEARABLE,
FLEXIBLE PULSE OXIMETER**

**A Thesis Submitted to
The Graduate School
İzmir Institute of Technology
in Partial Fulfillment of the Requirements for the Degree of**

MASTER OF SCIENCE

in Photonics Science and Engineering

by

Ahmed AYDIN

December 2020

İZMİR

ACKNOWLEDGMENTS

I would like to offer my profound gratitude to the people who contributed and assisted me for realizing this thesis.

- I am notably indebted to my supervisor, Assoc. Prof. Dr. Hüseyin Cumhuri Tekin, for giving me guidance, support and comprehension through this study.
- I would also like to thank to Izmir Institute of Technology Scientific Research Projects Coordinatorship (Project number: IYTE0284) for making great contributions to the realization of this study.
- Finally, to my parents and brothers for their ceaseless support.

ABSTRACT

DESIGN AND FABRICATION OF A WEARABLE, FLEXIBLE PULSE OXIMETER

Oxygen is vital for the healthy functioning of tissues and organs. For this reason, it is indispensable to monitor the oxygen saturation of the human body during daily activities in order to improve the quality of life, in the detection and tracking of respiratory diseases. Pulse Oximeter is an electro-optic device that non-invasively measures peripheral oxygen saturation and provides information about how well oxygen diffuses the tissues. Conventional devices are not suitable for daily use due to their bulky structure and designs that restrict movement. With this thesis, the design and production of a flexible reflectance type Pulse Oximeter device that is conformally adapt to measurement suite, can be used all day long and is intended for continuous measurement has been realized.

This thesis deals with a flexible Pulse Oximeter design, suitable for measurement from the fingernail and earlobe suites, that is produced by experimenting fabrication methods which do not require a clean room environment . Biocompatible and breathable materials have been preferred for the encapsulation of the electronic layer and for adhering the device to the measuring point. In order to process and store the data from the device, an Arm Cortex M0 based development board was used and the data was transferred via the I²C (Inter Integrated Circuit) data protocol. Oxygen saturation and heart rate data obtained from the presented device were compared with two different commercial Pulse Oximeters.

ÖZET

ESNEK, GİYİLEBİLİR BİR PULS OKSİMETRE TASARIM VE ÜRETİMİ

Dokular ve organların sağlıklı bir şekilde fonksiyonlarını sürdürebilmeleri için oksijen hayati bir öneme sahiptir. Bu sebeple, klinik bir müdahale öncesinde ve sonrasında, astım ve hipoksi gibi hastalıkların tespitinde ve takibinde, yaşam kalitesini artırmak amacıyla günlük aktivite esnasında insan vücudundaki oksijen doygunluğunun takip edilmesi vazgeçilmez derecede öneme sahiptir.

Puls Oksimetre kandaki oksijen doygunluğunu noninvazif olarak ölçen ve oksijenin dokulara ne kadar iyi nüfuz ettiği hakkında bilgi veren elektro-optik bir cihazdır. Konvansiyonel aygıtlar gerek hantal yapıları gerekse hareketi kısıtlayıcı tasarımları sebebiyle günlük kullanıma uygun değildir. Bu tez çalışması ile konvansiyonel cihazların sahip olduğu dezavantajların ortadan kaldırılması, vücut ile uyumlu, gün boyu kullanılacak ve sürekli olarak ölçüm alınmasına yönelik esnek, reflektans tipinde bir Puls Oksimetre cihazının tasarım ve üretimi gerçekleştirilmiştir.

Bu tez, temiz oda ortamı gerektirmeyen fabrikasyon yöntemlerinin denenmesiyle üretilen, tırnak ve kulak memesinden ölçüme uygun boyutta esnek bir Puls Oksimetre tasarımı ile ilgilidir. Elektronik katmanın enkapsülasyonu ve cihazın ölçüm noktasına yapıştırılması için biyo-uyumlu ve nefes alabilen malzemeler tercih edilmiştir. Tasarlanan cihazdan elde edilen verilerin işlenmesi ve depolanması amacıyla Arm Cortex M0 tabanlı bir geliştirme kartı kullanılmış ve veriler I²C (Inter Integrated Circuit) veri protokolü aracılığı ile aktarılmıştır. Sunulan cihazda elde edilen oksijen doygunluğu ve nabız sayısı verileri iki farklı ticari Pulse Oksimetre cihazı ile karşılaştırılmıştır.

Dedicated to my beloved nephew Mustafa Asaf.

TABLE OF CONTENTS

LIST OF FIGURES	vii
LIST OF TABLES	viii
CHAPTER 1. INTRODUCTION	1
1.1 Motivation	3
1.2 Methods to Measure Oxygen Saturation	3
1.3 Principles of Pulse Oximetry	4
1.4 Types of Pulse Oximeter	8
1.5 Limitations of Pulse Oximeter	9
CHAPTER 2. MATERIALS AND METHODS	10
2.1. Materials	10
2.1.1 Consumables	10
2.1.2 Equipments and Softwares	11
2.2 Methods	11
2.2.1 Fabrication of Conducting Layer	11
CHAPTER 3. RESULTS AND DISCUSSION	18
3.1 Data Acquisition	18
3.2 Data Measurement	21
CHAPTER 4 CONCLUSION	23
BIBLIOGRAPHY	24
APPENDIX A CIRCUIT SCHEMATIC	28
APPENDIX B MATERIAL LIST	29

LIST OF FIGURES

<u>Figures</u>	<u>Page</u>
Figure 1.1. Oxygen transportation.	4
Figure 1.2. Absorption spectra of Hb and HbO ₂	5
Figure 1.3. Form of the PPG signal.	6
Figure 1.4. Modulation ratio versus Oxygen Saturation.....	8
Figure 1.5. Types of pulse oximeter.	8
Figure 2.1. Photoresist mask.....	12
Figure 2.2. Three layer structure of negative dry film photoresist..	12
Figure 2.3. Process of Negative Dry Film Photoresist(NDFP) Method.	13
Figure 2.4. Structure of Payralux.....	14
Figure 2.5. Conductive layer of wearable and flexible pulse oximeter.	14
Figure 2.6. Structure of wearable, flexible pulse oximeter.....	15
Figure 2.7. Fabrication process of wearable, flexible pulse oximeter.	16
Figure 2.8. Wearable, flexible pulse oximeter.....	17
Figure 3.1. Schematic diagram of sensor connection for data acquisition	18
Figure 3.2. Measuring flow diagram.	19
Figure 3.3. Raw signal acquired from IR channel.....	19
Figure 3.4. PPG stream	20
Figure 3.5. S _p O ₂ and Heart Rate Measurement.	21

LIST OF TABLES

<u>Tables</u>	<u>Page</u>
Table 1. Factors effecting pulse oximeter reading.....	9
Table 2. Benchmark test result of Flexible Pulse Oximeter (FPU) with two commercial devices.....	22

CHAPTER 1

INTRODUCTION

Wearable devices have paved the way of revolutionizing personalized health with sensor applications including, tracking and recording of vital signs such as; heart rate, blood pressure, respiration rate, body temperature, oxygen saturation (S_pO_2) of users with the propose of leveraging their health. Due to their portability and wieldy, these devices took place in the market in the form of accessories and smart textiles like; smart watches^{1,2}, glasses^{3,4}, contact lenses⁵⁻⁹, earphones¹⁰, earrings^{11,12}, headsets¹³, wristbands^{14,15,16} and garments^{17,18}. The advancements in functional materials and manufacturing technologies cleared the way for researchers for embedding and encapsulating optoelectronic and microelectronic sensors and components on flexible substrates to create biomedical patches¹⁹⁻²¹, bandages²², tattoos²³ and skin-like systems^{24,25}. Thereby, wearable devices that are easily adopt to the body, can be used all day long, and can be integrated into mobile platforms have started to take their places in our lives.

A general wearable, flexible bioelectronic device has layer stacked structure composed of substrate, conductive interconnects, circuit elements and encapsulant layer. Substrate is the supporting layer that carries the entire system and provides mechanical robustness against deformation. Optical clearance, mechanical, thermal and chemical resistance, flatness, ruggedness and ease of handling are the parameters considered choosing the proper substrate for application specific devices. Polyethylene teraphthalate (PET), Polyethylene naphthalate (PEN), Polycarbonate (PC), Polyimide (PI), Polyarylate (PAR), Polycyclic olefin (PCO), Polynorbonene (PNB), Polyester are the most commonly used substrate materials due to their transparency and rollable/foldable feature. For the processes those require high heat, Polyimide(PI), Polyether sulphone (PES), Polyarylate (PAR), Polycyclic olefin (PCO), Polynorbonene (PNB) are the most preferred substrate materials due to their temperature resistance reaching $350^{\circ}C$ ²⁶⁻³² Encapsulant is the packaging layer protects the components from corrosion and provides a conformal contact between electronic components and human skin. As it is the contact layer between human skin and electronic components, encapsulant material has to be

biocompatible, anti-allergic and vigorous to elude physical failure incurred numerous human motions. Ecoflex, Sylgard 184, Dragonskin, Solaris, Silbione are the highly favored low modulus elastomeric encapsulant materials due to their biocompatibility and easy processability. In skin-like systems, organic and plastic derivative materials give way to elastomeric materials, Thermoplastic Polyurethane (TPU), Polyurethane (PU), medical grade tapes and water-soluble tapes.

In order to render flexible bioelectronic device, it is crucial to design sturdy conductive interconnects that stands distortion and provides stable signal transmission between components. For that purpose, two main design strategies became prominent: using intrinsically flexible conductors and tailored geometries of bulk metals in mesh, serpentine and wavy shapes. Gravure, offset, stencil, flexographic, inkjet, Microcontact & Nanoimprint printing for ink and paste form conductors, Chemical Vapor Deposition (CVD) and Physical Vapor Deposition (PVD) for bulk metals are the methods most widely used for creating conductive layer.

As one of the inevitable devices used for monitoring vital functions, Pulse Oximeter has made great improvements since Takuo Aoyagi's invention in 1972 and has reached a wide range of uses from ambulances to intensive care units, from surgery rooms to hyperbaric oxygen therapy centers. In recent years, developments in the field of wearable technologies have separated these devices from their rigid, cumbersome forms and moved them to forms that have mechanical compliance with human skin and that can be used all day long. Unlike the previous portable size variants of pulse oximeters, Haar *et al.* developed the first patch type reflectance oximeter with integrated battery and wireless communication feature³³. Since the location limitations of transmission type oximeter and advancements in flexible, conformal bioelectronics contributed an inviting path for developing organic, inorganic based oximeters. Lochner *et al.* developed all organic disposable oximeter³⁴. Yokota *et al.* reported the ultra-flexible and ultrathin skin-like reflectance oximeter that has polymer light emitting diodes (PLEDs) and organic photodetectors (OPDs)³⁵. Kim *et al.* developed a miniaturized oximeter by embedding electronic components into elastomeric encapsulants that operates up to three months.³⁶

The outline of this thesis begins with an introductory chapter, concerning the motivation, methods to measure oxygen saturation, limitations of pulse oximeters, types of pulse oximeters followed by working principles of pulse oximeter. In the next chapter, hardware design of the device utilized to control the prototype, fabrication method and

materials used to develop flexible pulse oximeter are presented. Finally, a discussion of the results and future directions are conversed.

1.1. Motivation

Oxygen is indispensable for energy production, nourishment and regeneration of cells and tissues. For this reason, the percentage of oxygenated hemoglobin in a living's blood gives direct information about the health and the state of the respiratory system. The recent outbreaks of Severe Acute Respiratory Syndrome (SARS) and the Middle East Respiratory Syndrome (MERS)^{37,38}, which have tragically affected the whole world and directly affect the respiratory system of the living, have shown us how important it is to monitor the oxygen level regularly and continuously. The current devices developed to monitor such a vital parameter are not suitable for use in daily life and harsh environments. For this reason, the need for an ergonomically and economically designed, and biocompatible pulse oximeter device that can be used throughout the day has increased.

1.2. Methods to Measure Oxygen Saturation

There are three main methods for measuring blood oxygen saturation: Transcutaneous Oximetry ($T_{cp}O_2$), Arterial Blood Gas Analysis (ABGA) and Pulse Oximetry. Transcutaneous Oximetry is a non-invasive, clinical grade method states the local oxygen level of tissue right below the skin³⁹⁻⁴¹. This technique quantitatively measures the oxygen delivery with the metal electrodes heated up to 44 °C to mitigate the vessels to increase the oxygen permeability under the skin. Although it is a clinically proven method, it requires trained personnel, hospital conditions, an environment above room temperature, 10-15 minutes to start measurement and calibration in every 4-8 hours in order to take a reliable measurement⁴². ABGA is another gold standard for measuring oxygen saturation of blood. In this method, a trained staff takes blood samples invasively in hospital environment for analysis. As a result of the analysis, this method provides important information such as oxygen saturation in the blood, Ph value of blood, partial pressure of Oxygen (P_aO_2) and partial pressure of Carbon dioxide (P_aCO_2). Although the ABGA method offers more information than other methods, the data is not real-time^{43,44}. Pulse Oximetry is a non-invasive method used to extract Peripheral Oxygen Saturation

(S_pO_2) and Heart Rate (HR). It works on the principle of different absorptivity of oxygenated hemoglobin (HbO_2) and deoxyhemoglobin (Hb). Unlike the other methods, Pulse Oximetry does not require a trained personnel and hospitalized environment. Although pulse oximetry generates less information than other methods, its repeatability, continuous and real-time measurement ability, and simplicity make it ahead of other methods.

1.3. Principles of Pulse Oximetry

Oxygen is transported through tissues and cells via hemoglobin. Hemoglobin is an iron-containing pigment that exist in Red Blood Cells (RBC) (Figure 1-a). During the respiratory cycle (Figure 1-b), hemoglobin conveys the oxygen molecules through body and then transmits the carbon dioxides depart from the cells and tissues to the lungs to be breath out. As the substantial majority of oxygen is sent through the body via hemoglobin, it could be presumed that oxygen content of red blood cell is a great illustration of standard blood oxygen saturation⁴⁵.

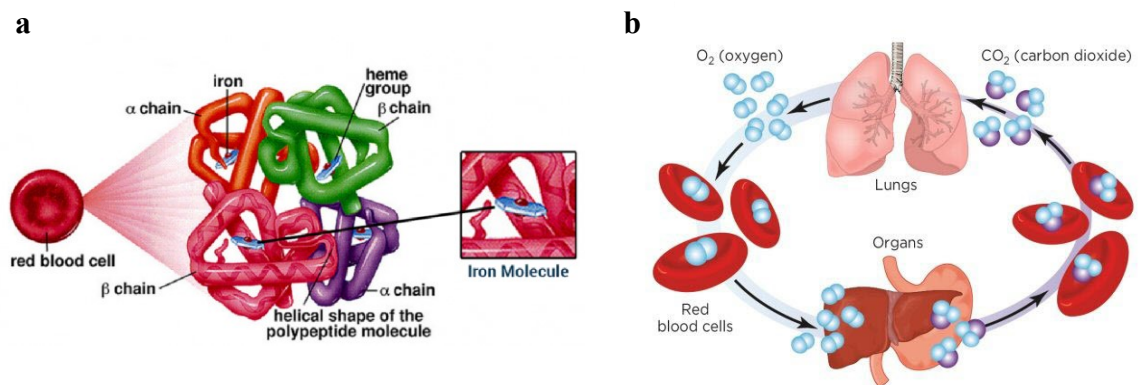


Figure 1.1. Oxygen transportation. (a) Illustrations of the red blood cell containing hemoglobin and (b) respiratory cycle (From reference 46).

Spectral absorbance of HbO_2 and Hb shows the significant difference in Red and slightly less distinction in IR region (Figure 1.2). While HbO_2 absorbs greater amount of IR light and lower amount of red light, Hb absorbs greater amount of Red light and lower amount of IR light. Exploiting the different light absorptivity of oxygenated and deoxygenated hemoglobin, pulse oximeter operates with 2 LEDs ; Red at $\pm 660nm$, IR at $\pm 940nm$ and a photodetector.

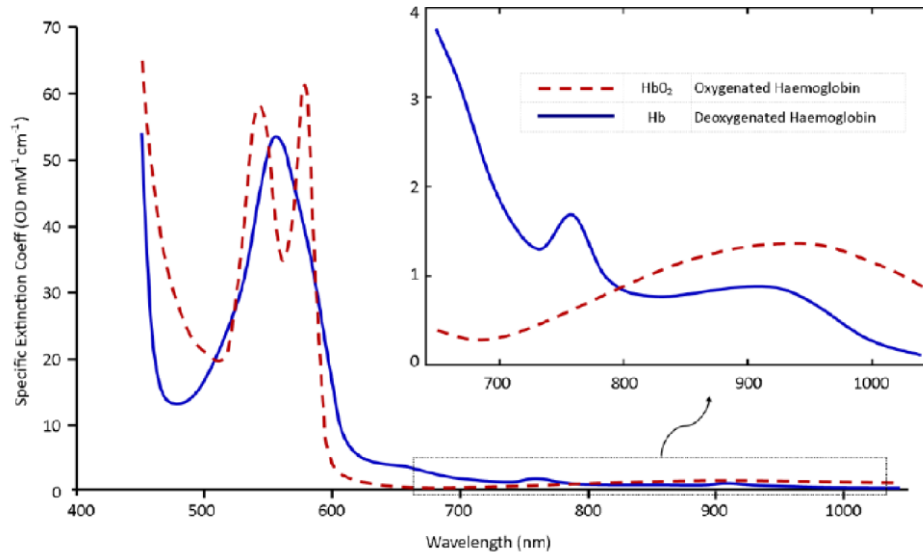


Figure 1.2. Absorption spectra of Hb and HbO₂ (From reference 48)

LEDs of Pulse Oximeter successively glow the tissue. Unabsorbed light strikes the photodetector, accordingly creates a signal in the form of photoplethysmography (PPG) (Figure 1.3). During cardiac cycle, arterial blood volume increases with systole and decreases with diastole. In contrast, the blood volume of capillaries, skin, fat, bone, etc. remains constant. The blood volume which rises with systole comprise the pulsatile or alternating (AC) part of the signal, the compartment which does not change during the cardiac cycle comprises the non-pulsatile (DC) component of the PPG signal.

The blood volume which rises with systole comprise the pulsatile or “ Alternating (AC) “ part of the signal, the compartment which does not change during the cardiac cycle comprises the non-pulsatile “ Direct (DC) ” component of the signal. PPG signal is processed relying on Beer-Lambert’s law which states absorbance of light that passes through a medium is proportional to the thickness of the sample and absorbent concentration⁵⁰. Derivation of Beer-Lambert’s law expressed with Equation 1.

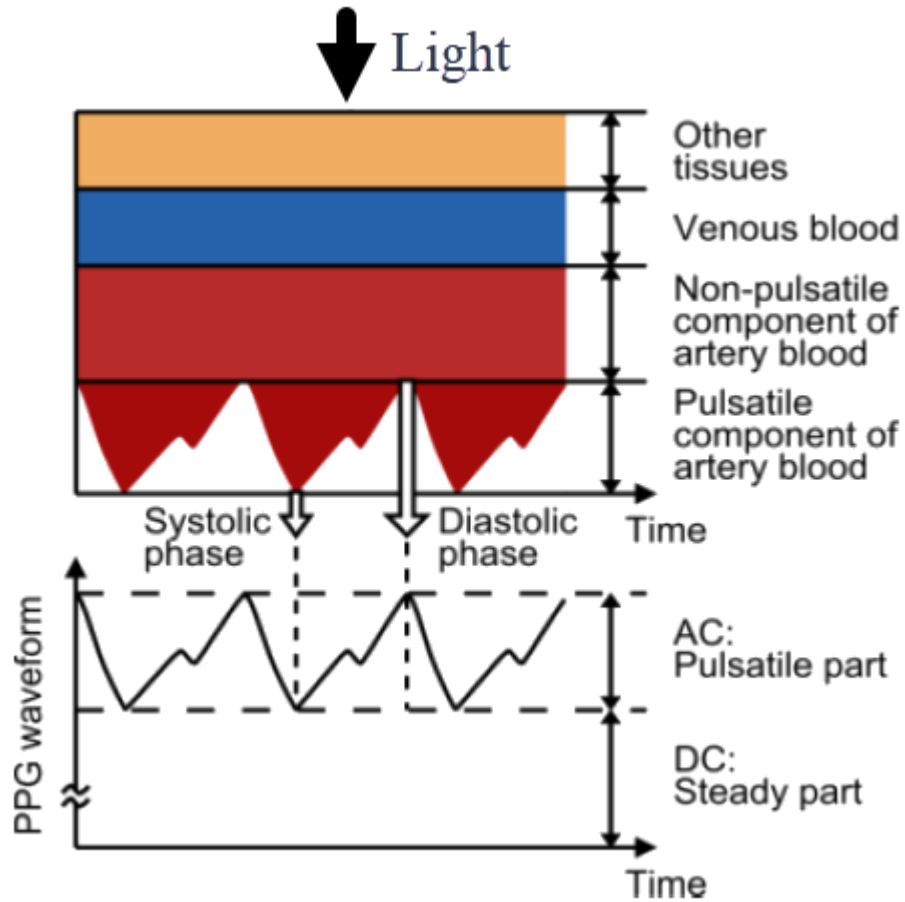


Figure 1.3. Form of the PPG signal. Adapted from (From reference 49)

$$I_t = I_o * 10^{-\alpha.d.c} \quad (\text{Equation 1})$$

, where I_t is intensity of transmitted light, I_o is intensity of incident light, α is extinction coefficient, d is optical path length and c is the concentration of sample.

Although, in a non-scattering medium equation-1 is valid for a single absorber, it is far from veracity. Because blood constitutes dysfunctional hemoglobin that interacts with light and affects the correct measurement. For that reason, Beer-Lambert's law need to be modified for multiple absorbents⁵¹ as given Equation 2.

$$A = \log_{10} \left(\frac{I_o}{I_t} \right) = [\alpha_1 c_1 + \alpha_2 c_2 + \dots + \alpha_n c_n] * d \quad (\text{Equation 2})$$

, where A is attenuation of light at a given wavelength, I_o is Intensity of incident light, I_t is Intensity of transmitted light, c is Concentration of compound, α is Extinction coefficient and d is the Optical path length.

It can be foreseen from the equation-2, modified Beer-Lambert's law need to be solved for five different variables which are highly dependent on specific wavelength. Moreover, the device itself requires correct calibration for different skin pigments and thickness those makes use of oximeter ineffective. In order to overcome aforementioned problems, a bioengineer from Nihon Kohden Company, Takuo Aoyagi invented ratio of ratios principle. In this principle, Takuo Aoyagi obtained a ratio R by dividing each wavelength to its corresponding AC and DC components which are independent of all factors those require calibration⁵¹:

$$R = (AC_r/DC_r)/(AC_{ir}/DC_{ir}) \quad (\text{Equation 3})$$

,where R is the double ratio of absorbance of pulsatile(AC) and non-pulsatile parts(DC) of the red I and infrared light (ir). This normalized ratio is associated with blood oxygen saturation with the formula given in Equation 4⁵¹:

$$S(t) = \frac{\alpha_{ir,ox} - \alpha_{ir,deox} * R(t)}{-(\alpha_{r,ox} - \alpha_{r,deox}) + (\alpha_{r,deox} - \alpha_{r,deox}) * R(t)} \quad (\text{Equation 4})$$

,where $S(t)$ is blood oxygen saturation, $\alpha_{ir,ox}$ and $\alpha_{ir,deox}$ are specific absorption coefficients of oxygenated and deoxygenated hemoglobin at infrared light respectively and $\alpha_{r,ox}$ and $\alpha_{r,deox}$ are specific absorption coefficients oxygenated and deoxygenated hemoglobin at red light respectively.

The relationship between modulation ratio and oxygen saturation is illustrated by calibration curve. In order to determine the oxygen saturation, oximeter quantifies the Ratio of Ratios value and evaluates the corresponding oxygen saturation from the curve given in Figure 1.4.

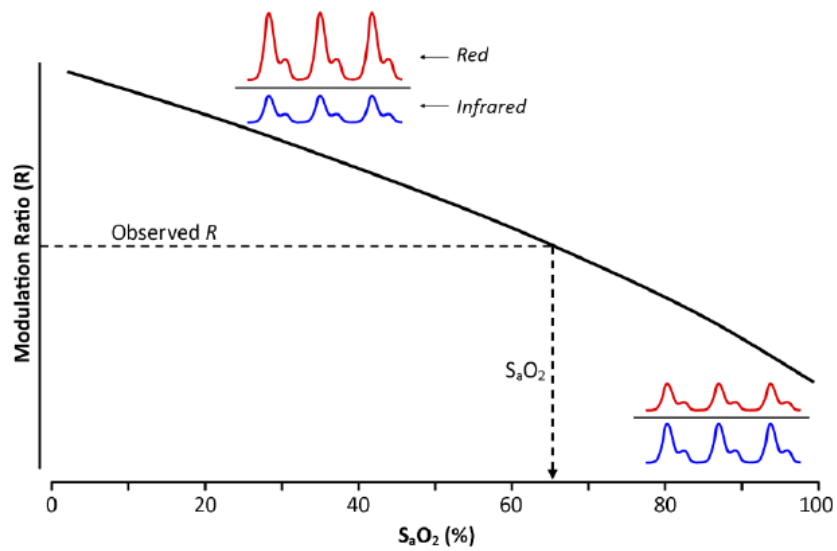


Figure 1.4. Modulation ratio versus Oxygen Saturation (From reference 52)

1.4. Types of Pulse Oximeter

Depending on the arrangement of LEDs and photodetector pulse oximeters are classified as reflective and transmissive. While, in transmissive type pulse oximeters LEDs and photodetectors are placed opposite side of measurement site (Figure 1.5-a), in reflective type oximeters they are positioned in the same side (Figure 1.5-b). Transmissive type oximeter requires a clean, thin measurement bed, such as finger, toe and ear. Nevertheless, reflective type oximeters are able to take measurement from wrist, forehead, chest and feet (newborn).

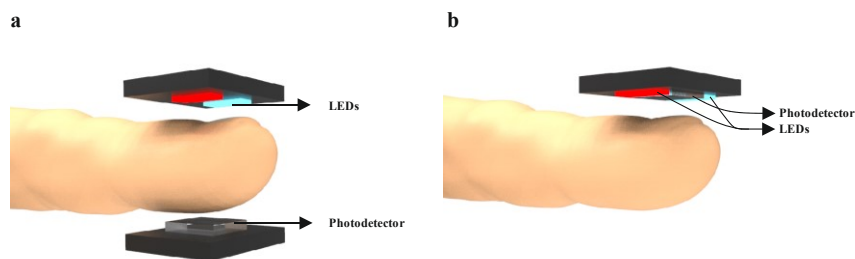


Figure 1.5. Types of pulse oximeter. a-) Transmissive pulse oximeter. b-) Reflective pulse oximeter.

1.5. Limitations of Pulse Oximeter

Due to their wiely, non-invasiveness and accuracy pulse oximeters took their places in our life. These electro-optic devices do not need any user calibration. But, there are several factors and limits arising from the measurement technique of device need to know by users for correct interpretation of data provided by device. Factors which cause erroneous oximetry reading listed in Table 1.

Table 1. Factors effecting pulse oximeter reading^{53,54}

Factors	Effects on Pulse Oximeter
Cardiac arrest	Poor signal
Respiratory arrest	Poor signal
Shock	Poor signal
Carbon monoxide poisoning	False increase in reading, often reading 100%
Cardiac arrhythmia	Poor signal
Dark skin	No interference
Peripheral vasoconstriction	Poor signal
Poor signal	Poor signal
Arteriovenous fistula	Poor signal
Nail polish	Poor signal with black, green, blue polish
Bright light or sunshine	False increase in signal (overreading)
Cold room	Poor signal
Electrical frequencies	Interference with signal
Shivering, tremors, rigors, motion	Poor signal
Dirty sensor	Poor signal

CHAPTER 2

MATERIALS AND METHODS

2.1. Materials

2.1.1. Consumables

The first prototype developed to verify the circuit design was built on FR4 PCB. This 1.6mm thick PCB has a 35um thick copper layer. The design validated on FR4 PCB was transferred onto flexible PCB material (Pyralux AC 352500EY, Dupont, U.S.A) to separate and clean the copper surface from the oxide layer, Brasso copper polisher (RB, U.S.A), Isopropanol (VWR International, U.S.A), Acetone (VWR International, U.S.A) and pure water were used, respectively, and the samples were dried with nitrogen gas (Gunes Gas, Turkey). Thermal Release Tape (Xiomen Kingzom, China) was used to prevent deformation of the flexible PCB material during cleaning process. The circuit design was transferred onto the flexible PCB via Negative Photoresist film ((Shenzhen Sunshine, China)). After UV exposure, sodium carbonate (AS Kimya, Turkey) was used for photoresist development. A mixture of Hydrochloric Acid (37%, Akbel Kimya, Turkey) and Hydrogen Peroxide (50%, Akbel Kimya, Turkey) were used for chemical etching. For the soldering of electronic components on the circuit, non-marking flux (Soldex, Turkey), low-melting point solder (NeVo, PF602-P26, Germany) and a 120 micron thick stencil sieve were used (Sparks, İzmir). After the soldering process, the circuit board was cleaned with Kontakt PCC (Kontakt Chemie, Germany). The cables used for data transfer from the circuit board were coated with insulating spray (Bionertech, Turkey). Polydimethylsiloxane (PDMS) (Sylgard 184, Sigma Aldrich, Germany) was used for the encapsulant layer of the pulse oximeter. Teflon spray (Winkel, Turkey) was used to easily separate the encapsulant layer from the clear resin mold (FLGPCL02, Formlabs, U.S.A). Surgiseal Stylus (Adhezion Biomedical LLC, UK) and medical grade double sided tape (3M 1567, U.S.A) were used to attach the first wearable and flexible pulse oximeter device to the nail.

2.1.2 Equipments and Softwares

During the fabrication process, the Silhouette Cameo 3 desktop plotter was used to cut Pyralux flexible PCB material and negative photoresist. A 4-roller laminator device (Mühlen Elegant LM-330DN, Germany) was used for mask and photoresist lamination. A UV lamp (JD-818, China) was used to polymerize the photoresist. For the PDMS encapsulant mold Formlabs Form 2 Desktop-SLA 3D printer (Formlabs, USA) were used. Precision balance (Kern PLJ, Germany), one stage vacuum pump (Aitcool, China) and Incubator (Mettler, Germany) were used to weigh, degas and cure the PDMS, respectively. A Digital Multimeter (UNI-T, UT139) was used to test the continuity of the current paths of the flexible circuit board. A heat gun was used for soldering (Yihua 8858, China) and a stereo microscope (Carl Zeiss, Stemi 508, Germany) was used for inspections. The Adafruit Feather M0 (Adafruit Industries, U.S.A) development board was used to process the data obtained from the wearable, flexible pulse oximeter, and a 16Gb SD card (Sandisk Ultra) was used to save the data. Student versions of Autodesk Autocad and Fusion 360 software were used for technical drawing and 3D design. Preform 3D printer slicer software was used for 3D mold printing. Altium Circuit Studio was used for electronic design. A handheld (Galena PC66B) and finger-type pulse oximeter were utilized to compare the flexible and wearable pulse oximeter that was designed and manufactured in this thesis.

2.2 Methods

2.2.1 Fabrication of Conducting Layer

A single layer hardware was designed using the smallest components that can be soldered by hand, following the manufacturer's recommendations. MAX30102EFD + pulse oximeter sensor from Maxim Integrated company was used in the design. The sensor with 2 LEDs(λ_{red} : 660nm, λ_{ir} : 880nm), 1 photodetector that has a spectral range between 600-900nm and internal Analog to Digital Converter (ADC) communicates over I²C protocol.

Sensor operates on a single 1.8V power supply and 3.3V power supply for internal LEDs. In order to provide a constant power that sensor requires, 3.3V and 1.8V voltage regulators were used (Appendix B). The device itself is able to operate with 3.3V and 5V. The schematic (Appendix A) and PCB design of the device was carried out with Altium Designer Circuit Studio.

The conductive layer of the design was exported as dxf file format to use as a mask in the Negative Dry Film Photoresist (NDFP) method and edited with Autodesk Autocad (Figure 2.1).

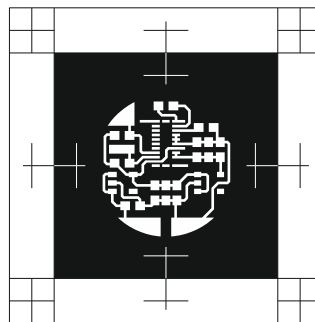


Figure 2.1. Photoresist mask. Each trace has 300um width. Pads for power supply and I2C (SDA,SCL,INT) have 1.5mm by 1.5mm dimensions

Negative dry film is a photosensitive which is used to create resistive layer against chemical etchant. It is comprised of 3 layers (Figure 2.2). The blue photosensitive layer (38 μ m), that is in the middle layer, is the polymer layer which hardens and resist against etchant when exposed to UV-light. The other two layers (25 μ m) are protective transparent layers in bottom and top sides.

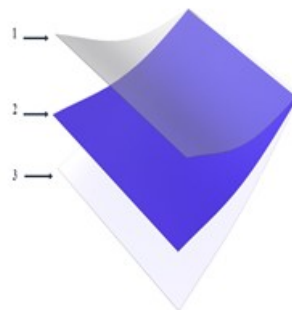


Figure 2.2. Three-layer structure of negative dry film photoresist. Layer one is the top protective PET layer (25 μ m), Layer two is the photosensitive layer (38 μ m), and Layer three is the protective PE layer (25 μ m).

In the Negative Dry Film Photoresist method, the desired patterns are printed on the transfer surface by using a thin film layer sensitive to ultraviolet light. The process begins by covering the substrate with negative photoresist dry film. A mask is then applied to the surface to block the light so that only the unmasked areas of the material are exposed to the light. Parts exposed to light polymerize and harden. Later, when this surface is released into the developer, the areas not exposed to light are separated from the surface (Figure 2.3).

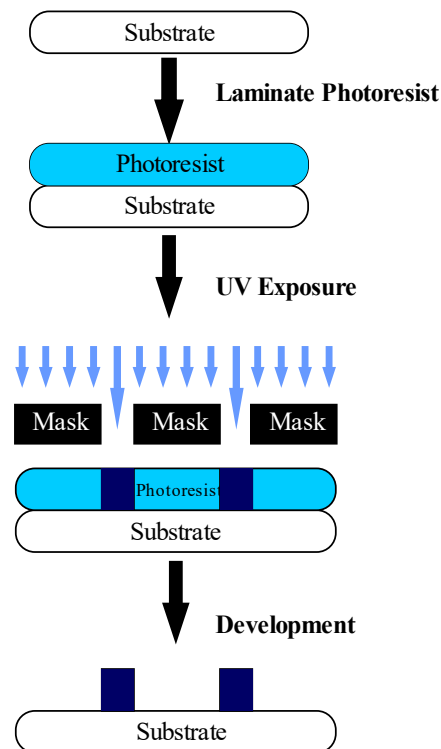


Figure 2.3. Process of Negative Dry Film Photoresist(NDFP) Method.

Steps of Photosensitive Dry Film Fabrication Process include:

- Mask design
- Cleaning copper surface
- Lamination of photosensitive negative dry film (110°C, 3 times lamination)
- Mask alignment
- UV-light exposure
- Development (%1 Sodium Carbonate)
- Chemical etching (H_2O_2 (%50) + HCl (%37), 1:5)
- Cleaning

Pyralux is a bi-layer copper clad laminated flexible PCB material that constitutes the substrate and conductive layer of the device (Figure 2.4).

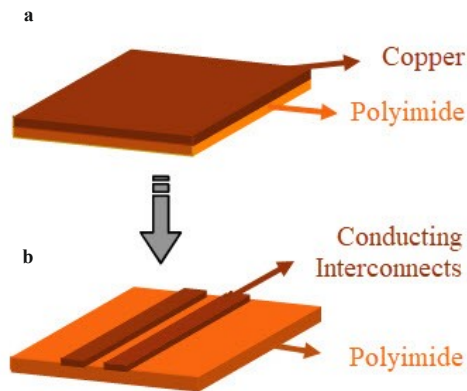


Figure 2.4. Structure of Payralux. A-) Pyralux AC 352500EY is a bi-layer flex PCB material with $35\mu\text{m}$ copper and $25\mu\text{m}$ polyimide thickness. B-) Copper interconnects obtained after NDFP method.

The method used to obtain the conductive layer determines the fabrication method of the device. As outlined above, the Negative Dry Film Photoresist method was used to create the conductive layer (Figure 2.5). With this method, fair resolution was obtained for the designed circuit ($100\mu\text{m}$ line width, $100\mu\text{m}$ space with adjacent lines).

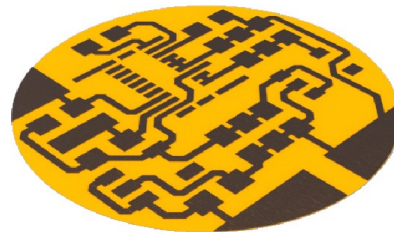


Figure 2.5. Conductive layer of wearable and flexible pulse oximeter.

The wearable and flexible pulse oximeter have layer stacked structure and composed of five layers (Figure 2.6). Layer one is the adhesive layer that is used to stick the device on skin. A medical grade and breathable double-sided tape (3M 1567) was used in this layer. Layer two is the top and bottom encapsulant (Sylgard 184, Dow Corning) which provides a soft interface between device and human skin and mechanical resistance against deformation. Layer three is the component layer. Components are

connected to the conducting layer via low melting point solder (NeVo PF602-P26). Layer four is the conducting layer that is manufactured via NDFP method and responsible for signal transmission between components. Layer five is the polyimide substrate that carries entire system.

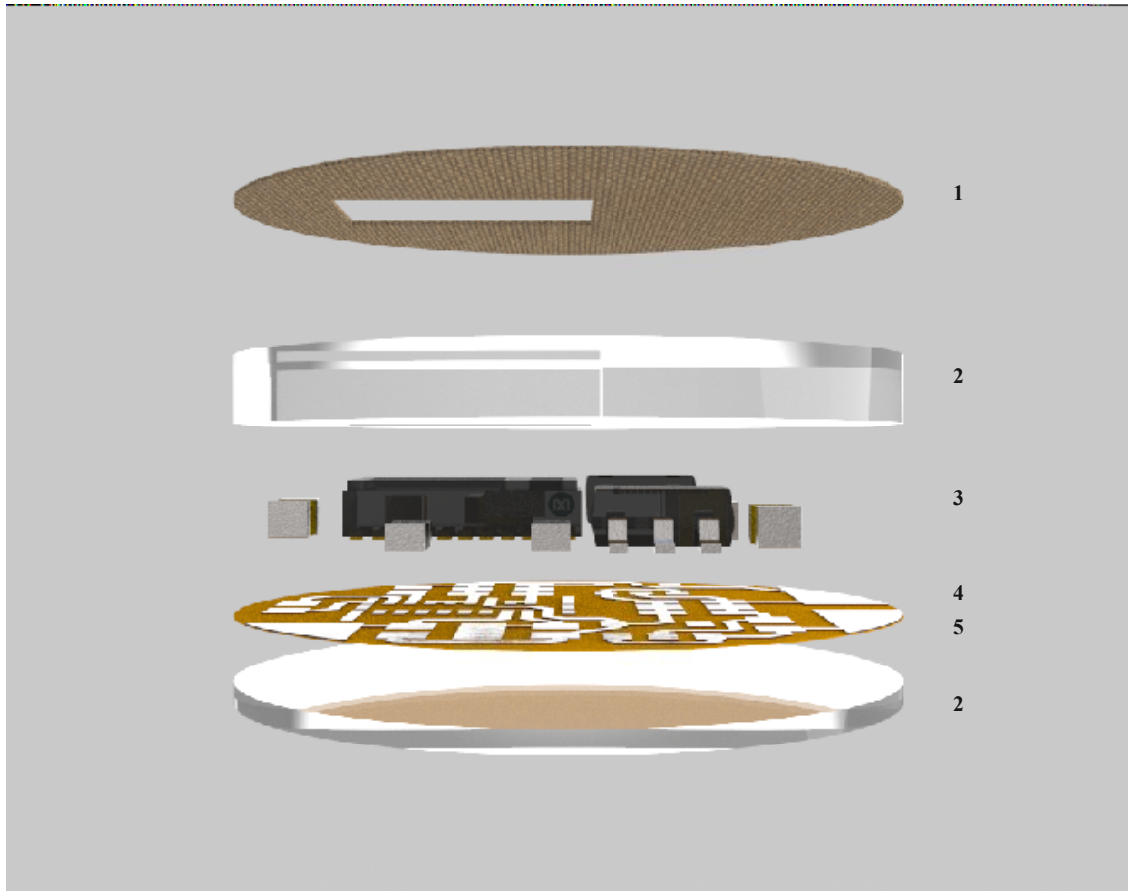


Figure 2.6. Structure of wearable, flexible pulse oximeter.

The manufacturing of the device has a fairly simple process as shown in figure 2.7. Pyralux cut in 3cm by 3cm dimensions with a desktop plotter device (Silhouette Cameo 3) is adhered to the Thermal Release Tape, which is cut in 5cm by 5cm sizes with the same device. The purpose of using Thermal Release Tape (TRT) here is to provide a flat base to pyralux which is highly susceptible to deformation. Then, NDFP is cut in 2cm by 2cm dimensions and is laminated (3 times at 120°C) on the copper surface of pyralux by Mühlen LM330DN (Figure 2.7-a). The required circuit design is obtained by following the photolithography processes by laminating the mask onto the prepared sample (Figure 2.7-b). After these processes, the conductive layer is cut with a 7.5mm radius using Epilog

CO₂ laser and the connections those required for the power supply of the device and data communication are obtained by engraving the polyimide layer with Epilog CO₂ laser (Figure 2.7-c). After these processes, the sample was cleaned with Isopropyl alcohol and distilled water, and the conductive layer was dried with nitrogen gas. Next, electronic components were soldered onto the conductive layer. Low temperature melting solder (NeVo PF602-P26) was applied on the circuit with a stencil. A hot air gun was used in the soldering process (Figure 2.7-d). The encapsulant layers of the device is prepared on the mold. Mold, which has a diameter of 1.5 cm and a depth of 1.6mm was prepared using Desktop-SLA 3D printer (Formlabs, USA) with transparent resin (FLGPCL02, Formlabs, USA). After the printing process, the mold was kept in isopropanol for 45 minutes and dried with nitrogen gas to remove the uncured resin. PDMS was used as the encapsulant material. PDMS prepared with a mixture ratio of 10: 1 (monomer: curing agent ratio). After degas treatment PDMS was poured into the mold and partially cured at 60 degrees for 2 hours in incubator (Mettler, Germany) (Figure 2.7-e). The cables were soldered to the connection points opened from the polyimide layer of the sample removed from the mold. Then, PDMS was poured onto the substrate of the sample placed in another mold which has a depth of 2mm, a diameter of 1.5cm and it was left to cure for 6 hours at 80°C in the incubator (Figure 2.7-f). Finally, the device taken from the incubator was ready for use (Figure 2.7-g).

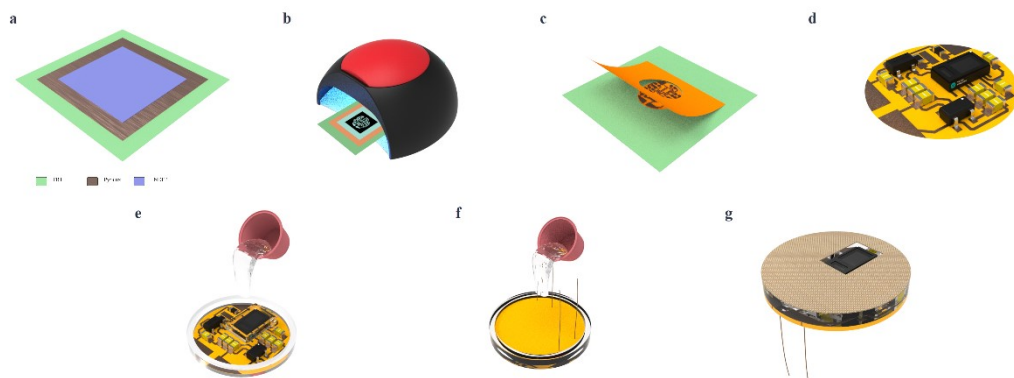


Figure 2.7. Fabrication process of wearable, flexible pulse oximeter. Pyralux's PI surface was placed on the TRT and NDFP laminated over the copper surface (a). The mask shown in Figure 2.1 was placed on the NDFP and photolithography, development, and chemical etching were performed (b). The excessive parts were removed with CO₂ laser cutter and the PI surface of Pyralux was rastered with a laser cutter by leaving a 1mm by 1mm opening for the I²C and power connections (c). After the electronic components were soldered (d), PDMS was poured on the 1.6mm deep and 1.5cm diameter mold to form the top layer of the device and cured in the oven I. After the curing of the upper layer, the device was placed in another mold with a depth of 2mm and 1.5cm in diameter in order to form the bottom layer of the device, PDMS was poured on it and cured in the oven (f). Finally, the device was made ready for use with its final shape (g).

The pulse oximeter produced using the aforementioned fabrication steps is 1.5cm in diameter and 2mm thick. This device, which can be bent (Figure 2.8-a), twist (Figure 2.8-b) and adapts comfortably to the skin (Figure 2.8-c), has been designed and manufactured for the use throughout the day.

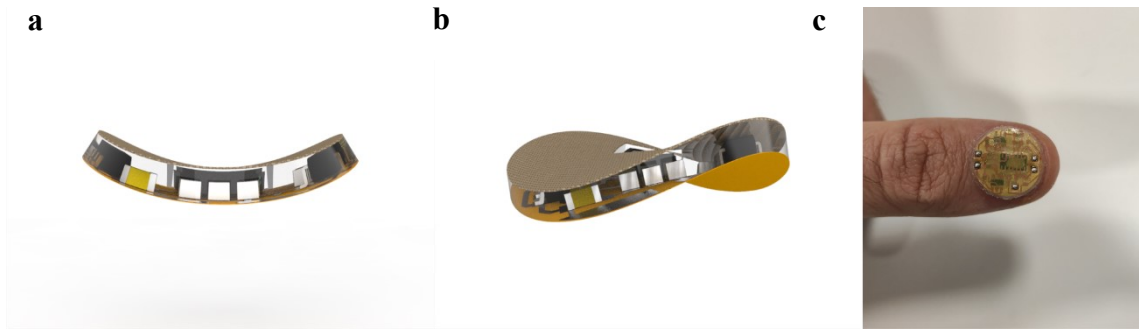


Figure 2.8. Wearable, flexible pulse oximeter a-) Bended 3D view b-) Twisted 3D view c-) Photograph of the device attached on a fingernail.

CHAPTER 3

RESULTS AND DISCUSSION

3.1 Data Acquisition

An ARM Cortex M0 based development board (Adafruit Adalogger M0) was used to acquire and process data from the manufactured flexible pulse oximeter. The power and communication connections between the development board and the sensor were made as shown in the figure below (Figure 3.1). The data processed on the development board was transferred to the computer via the Arduino IDE.

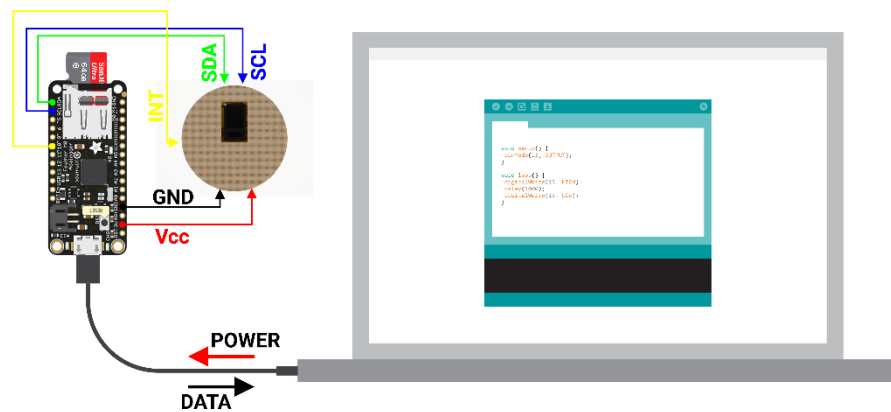


Figure 3.1. Schematic diagram of sensor connection for data acquisition

The principle of Puls Oximetry sensor operation is quite simple. Red (660nm) and IR (880nm) LEDs shine sequentially through tissue. The light is partially absorbed by underlying tissues together with peripheral blood. Photodetector collects the returning light in both wavelengths and reverts corresponding relative intensities with the help of I²C communication protocol. (Figure 3.2).

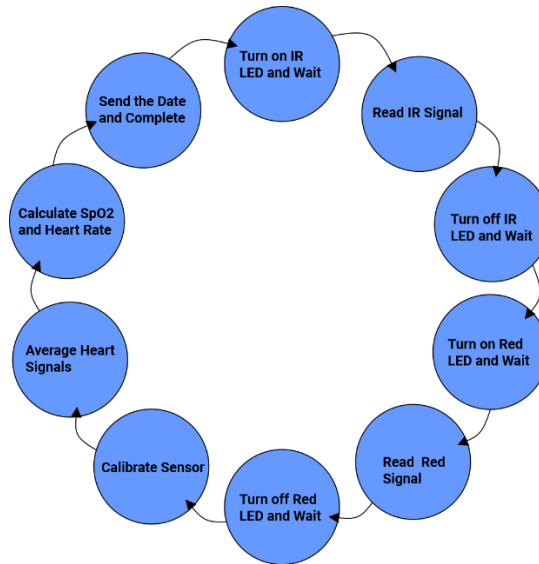


Figure 3.2. Measuring flow diagram.

Since absorption spectra for oxygenated and deoxygenated hemoglobin distinct for both wavelengths, the reflected light has a fluctuating component created with each heartbeat. Calculation of heart rate and oxygen saturation is conducted using the signal processing software and algorithm provided by the manufacturer. Figure 3.3 illustrates the raw signals obtained from IR led.

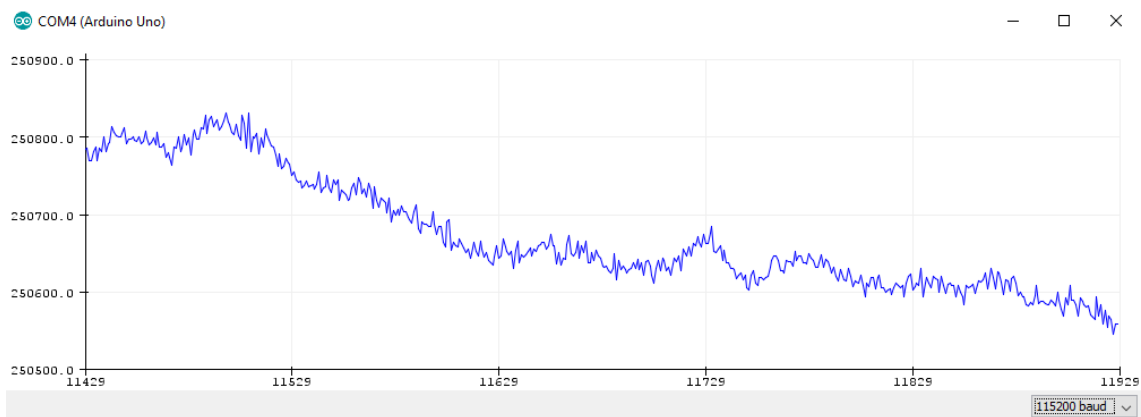


Figure 3.3. Raw signal acquired from IR channel

In the application, the raw data is collected at 25 Hz corresponds to 100 data points obtained within 4 seconds time period. The acquired data is processed in the software provided by the manufacturer to obtain a smooth PPG waveform. (Figure 3.4).

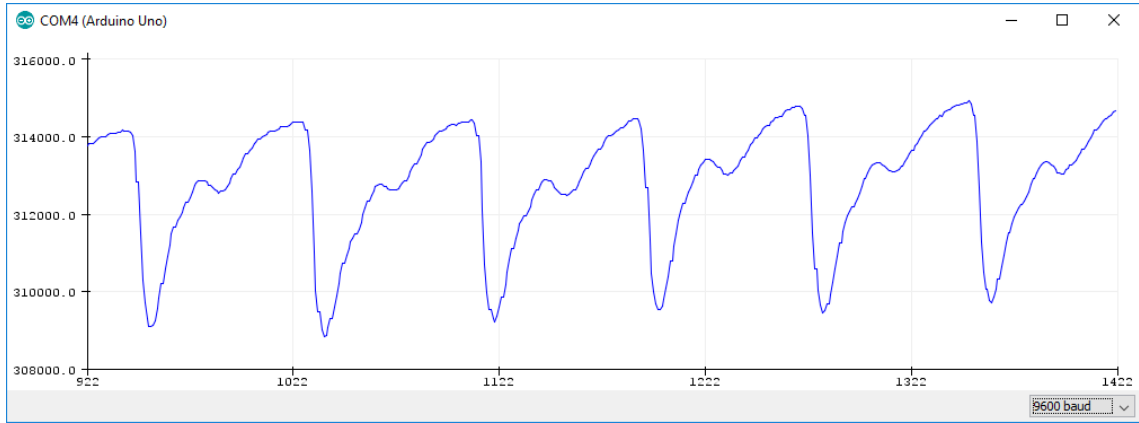


Figure 3.4. PPG stream

In order to determine the heart rate, sensor collects 25 data point in a second. Hence, the period in seconds corresponds to $m / 25$, where m is the time period. By this way, heart rate can be designated in beats per minute(bpm) by the formula in Equation 5.

$$H.R = 60 * \frac{25}{m} = \frac{1500}{m} \text{ (bpm)} \quad (\text{Equation 5})$$

In order to calculate the S_pO_2 value, the red LED, that is not used to calculate heart rate, should also be taken into account. S_pO_2 value is calculated with the formula provided by manufacturer shown in Equation 6:

$$SpO_2 = (-45.06 * R + 30.354) * R + 94.845 \quad (\text{Equation 6})$$

, where R is the ratio of ratios (Equation 3). Consequently, measurement results displayed via Arduino IDE console (Figure 3.5).

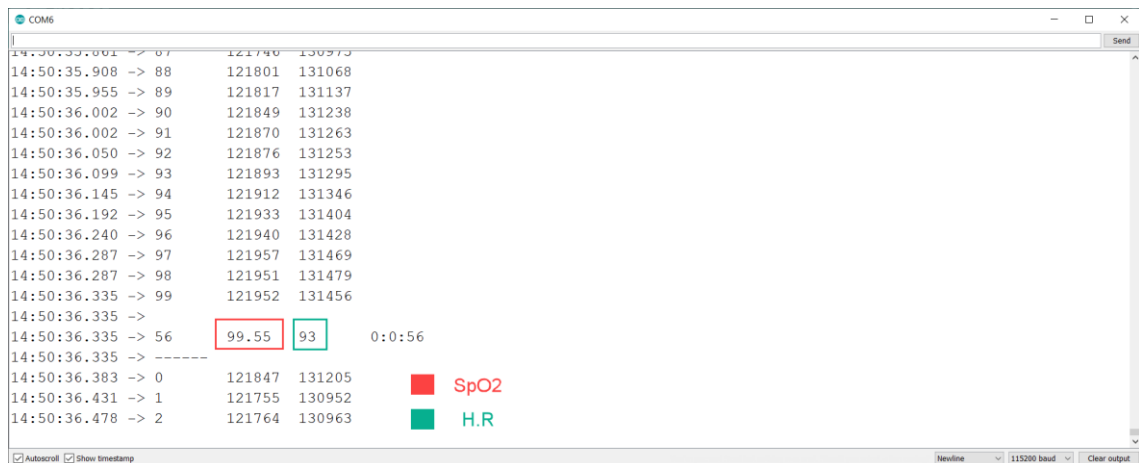


Figure 3.5. SpO₂ and Heart Rate Measurement.

3.2 Data Measurement

Pulse oximetry was developed with the presented method within the scope of this work. A benchmark test was performed with commercially available pulse oximeters to measure the accuracy of the flexible pulse oximeter. In this benchmark test, data were collected from ten different adults ages 25-65. Measurements were taken from the index fingers while sitting. The devices were set to take measurements every four seconds and the measurements were recorded for one minute. SpO₂ and Heart Rate (H.R.) values obtained from each subject were averaged at the end of one minute. The table below shows the data from these devices. Device 1, Device 2 and FPO represents the handheld, fingertip and flexible pulse oximeter respectively. While FPO showed similar results with Device 1 in H.R. and SpO₂ measurements, it showed similar results with Device 2 only in H.R. measurement. In SpO₂ measurement, the margin of error between FPO and Device1 and Device2 was determined as 1.63% and 12.11%, respectively, while the margin of error between FPO and Device1 and Device2 in H.R. measurements was 0.24% and 0.70%, respectively.

Table 2. Benchmark test result of Flexible Pulse Oximeter (FPO) with two commercial devices.

Subject	Device 1		Device 2		FPO	
	S _p O ₂	H.R.(bpm)	S _p O ₂	H.R.(bpm)	S _p O ₂	H.R.(bpm)
1	99	96	96	95	97	97
2	98	82	95	84	96	81
3	99	80	96	76	97	80
4	98	94	95	97	96	94
5	99	71	96	74	97	72
6	99	89	96	88	97	89
7	98	84	95	86	96	83
8	98	74	95	75	96	74
9	95	94	96	98	94	95
10	96	87	98	86	99	88

CHAPTER 4

CONCLUSION

The aim of this thesis is to design a wearable, flexible and miniature device without using clean room processes, expensive equipments and long-processing times, which are frequently preferred in the literature, and to use it as a bio-electronic sensor. As an alternative to metal evaporation methods, the "Negative Dry Film Photoresist" method, which allowed to reach 100 μ m line thickness, was chosen to fabricate the presented device.

Although the device was designed as 1.5 cm in diameter, its diameter can be reduced to less than 1 cm by using 0402 package electronic components instead of 0603 package. The device works with approximately 2% margin of error when compared to commercial devices. In order to reduce this error, the algorithm of the device needs to be improved. The device needs to be compared with also Nellcor compatible devices. Although the device wraps the curvature of the nail harmoniously, the degree of bendability needs to be tested on the device.

In the future, it is aimed to move the device to a mobile platform that can wirelessly communicate, operate without a battery and measure body temperature as well as S_pO_2 and Heart Rate measurements. Thus, the device will become capable of taking measurements from the fingertip, forehead, wrist and earlobe, which can be used all day, and inform the user via a mobile phone that could be used for COVID-19 monitoring also.

BIBLIOGRAPHY

- [1]<https://www.wearable-technologies.com/gadgets-of-the-month/12dec-basic> Wearable Tech. 2018. Basis Band B1–Health Tracker. (Access Time: 18.12.2020, 23:00)
- [2]Samsung 2015. Gear Fit. <https://www.samsung.com/us/support/owners/product/gear-fit>. (Access Time: 18.12.2020, 23:00)
- [3] Pu, Xianjie, et al. (2017) "Eye motion triggered self-powered mechnosensational communication system using triboelectric nanogenerator." *Science advances* 3.7: e1700694.
- [4] Hernandez, Javier, et al. 2014"Bioglass: Physiological parameter estimation using a head-mounted wearable device." 2014 4th International Conference on Wireless Mobile Communication and Healthcare-Transforming Healthcare Through Innovations in Mobile and Wireless Technologies (MOBIHEALTH). IEEE.
- [5] <https://www.magicleap.com/en-us> (Access Time: 18.12.2020, 23:00)
- [6] Elsherif, Mohamed, et al. (2018) "Wearable contact lens biosensors for continuous glucose monitoring using smartphones." *ACS nano* 12.6 5452-5462.
- [7] Chen, Guo-Zhen, et al. (2014) "Soft wearable contact lens sensor for continuous intraocular pressure monitoring." *Medical engineering & physics* 36.9 (2014): 1134-1139.
- [8] Kim, Joohee, et al. (2017) "Wearable smart sensor systems integrated on soft contact lenses for wireless ocular diagnostics." *Nature communications* 8.1 1-8.
- [9] Tseng, Ryan Chang, et al. (2018) "Contact-lens biosensors." *Sensors* 18.8: 2651.
- [10]Bragi. 2015. Dash Pro. <https://www.bragi.com/thedashpro/> (Access Time: 18.12.2020, 23:00)
- [11]Biosensive Tech. 2015. Ear-O-Smart. <http://earosmart.com/> (Access Time: 18.12.2020, 23:00)
- [12]Cosinuss One. <https://www.cosinuss.com/products/fitness/> (Access Time: 18.12.2020, 23:00)
- [13]<https://www.emotiv.com/epoc/> (Access Time: 18.12.2020, 23:00)
- [14]Wearable Tech. 2018. <https://www.wearable-technologies.com/store/phyode-w-me-wristband.html> (Access Time: 18.12.2020, 23:00)
- [15]<http://www.ihealthlabs.com/blood-pressure-monitors/wirelessblood-pressure-wrist-monitor> (Access Time: 18.12.2020, 23:00)

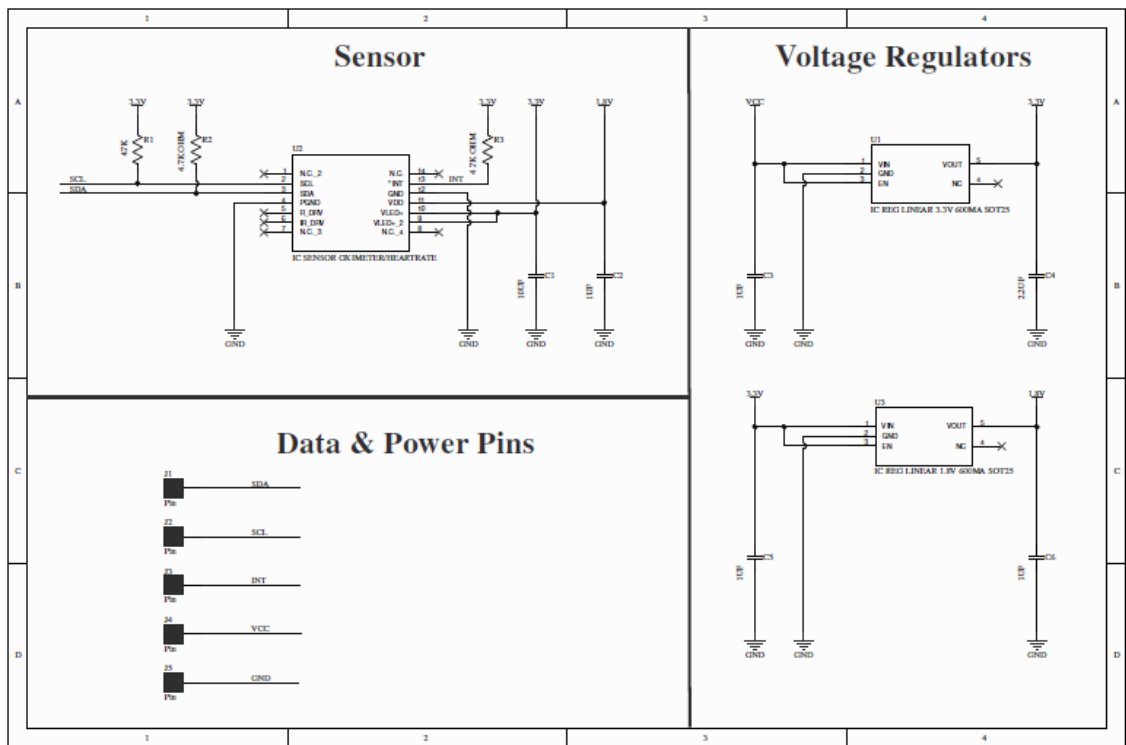
- [16]Omron 3 Series Wrist Blood Pressure Monitor. (Access Time: 18.12.2020, 23:00)
<http://omronhealthcare.com/products/3-serieswrist-blood-pressure-monitor-bp629/>
- [17]Jeong, J. W., et al. (2009)"Wearable respiratory rate monitoring using piezo-resistive fabric sensor." World Congress on Medical Physics and Biomedical Engineering, September 7-12, 2009, Munich, Germany. Springer, Berlin, Heidelberg.
- [18]Goode L. 2015. Ralph Lauren's 'smart' shirt is the ultimate preppy tech. Aug. 20.
<https://www.theverge.com/2015/8/20/9178923/ralph-laurens-polotech-smart-shirt-is-the-ultimate-preppy-tech>
- [19]<https://www.mc10inc.com/our-products> (Access Time: 18.12.2020, 23:00)
- [20]<https://www.laroche-posay.us/my-skin-track-uv-3606000530485.html> (Access Time :18.12.2020, 23:00)
- [21]Noh, S., et al. (2014) "Ferroelectret film-based patch-type sensor for continuous blood pressure monitoring." *Electronics letters* 50.3: 143-144.
- [22]Mostafalu, Pooria, et al. (2018) "Smart bandage for monitoring and treatment of chronic wounds." *Small* 14.33 :1703509.
- [23]Jeong, Hyoyoung, and Nanshu Lu. 2019 "Electronic tattoos: the most multifunctional but imperceptible wearables." *Smart Biomedical and Physiological Sensor Technology XV*. Vol. 11020. International Society for Optics and Photonics.
- [24]Liu, Yuhao et al. (2019) "Lab-on-skin: a review of flexible and stretchable electronics for wearable health monitoring." *ACS nano* 11.10 (2017): 9614-9635.
- [25]Rodrigues, Daniela, et al. (2020)"Skin-integrated wearable systems and implantable biosensors: A comprehensive review." *Biosensors* 10.7 (2020): 79.
- [26]Kaltenbrunner, Martin, et al.(2013) "An ultra-lightweight design for imperceptible plastic electronics." *Nature* 499.7459 (2013): 458-463.
- [27]Huang, Xian, et al. (2012)"Epidermal differential impedance sensor for conformal skin hydration monitoring." *Biointerphases* 7.1 (2012): 52.
- [28]Webb, R. Chad, et al.(2013) "Ultrathin conformal devices for precise and continuous thermal characterization of human skin." *Nature materials* 12.10 (2013): 938-944.
- [29]Jeong, Jae-Woong, et al. (2015) "Wireless optofluidic systems for programmable in vivo pharmacology and optogenetics." *Cell* 162.3 (2015): 662-674.
- [30]Choi, Myeon-Cheon et al. (2008) "Polymers for flexible displays: From material selection to device applications." *Progress in Polymer Science* 33.6 (2008): 581-630.
- [31]MacDonald, William A., et al. (2007)"Latest advances in substrates for flexible electronics." *Journal of the Society for Information Display* 15.12 (2007): 1075-1083.

- [32]Zardetto, Valerio, et al. (2011) "Substrates for flexible electronics: A practical investigation on the electrical, film flexibility, optical, temperature, and solvent resistance properties." *Journal of Polymer Science Part B: Polymer Physics* 49.9 (2011): 638-648.
- [33]Haahr, Rasmus G., et al. (2011) "An electronic patch for wearable health monitoring by reflectance pulse oximetry." *IEEE Transactions on Biomedical Circuits and Systems* 6.1 (2011): 45-53.
- [34]Lochner, Claire M., et al. (2014)"All-organic optoelectronic sensor for pulse oximetry." *Nature communications* 5.1 (2014): 1-7.
- [35]Yokota, Tomoyuki, et al. (2016) "Ultraflexible organic photonic skin." *Science advances* 2.4 (2016): e1501856.
- [36]Kim, Jeonghyun, et al. (2017) "Miniaturized battery-free wireless systems for wearable pulse oximetry." *Advanced functional materials* 27.1 (2017): 1604373.
- [37]Huang, Chaolin, et al. (2020) "Clinical features of patients infected with 2019 novel coronavirus in Wuhan, China." *The lancet* 395.10223 (2020): 497-506.
- [38]Wang, Dawei, et al. (2020) "Clinical characteristics of 138 hospitalized patients with 2019 novel coronavirus–infected pneumonia in Wuhan, China." *Jama* 323.11 (2020): 1061-1069.
- [39]Kmiec, Maciej M., et al. (2019) "Transcutaneous oxygen measurement in humans using a paramagnetic skin adhesive film." *Magnetic resonance in medicine* 81.2 (2019): 781-794.
- [40]Huch, R., D. W. Lübbers, and A. Huch. "Quantitative continuous measurement of partial oxygen pressure on the skin of adults and new-born babies." *Pflügers Archiv* 337.3 (1972): 185-198.
- [41]Huch, Renate, Albert Huch, and Dietrich W. Lübbers. "Transcutaneous measurement of blood Po₂ (tcPo₂)—method and application in perinatal medicine." (1973).
- [42]Kavassalis, Fivos I., Bill Chieng, and Franco Agustin Baudino. "Flexible Wearable Sensor." (2020).
- [43]Sood, Pramod, Gunchan Paul, and Sandeep Puri. "Interpretation of arterial blood gas." *Indian journal of critical care medicine: peer-reviewed, official publication of Indian Society of Critical Care Medicine* 14.2 (2010): 57.
- [44]K. Gaines, "Know your abgs - arterial blood gases explained." [Online]. Available: <https://nurse.org/articles/arterial-blood-gas-test/> (Access Time: 18.12.2020, 23:00)
- [45]Martini, F.H. & Bartholomew, E.F., 2007. *Essentials of Anatomy & Physiology*. San Francisco, CA, United States of America: Pearson Education Inc.
- [46]<https://askhematologist.com/abnormal-hemoglobins> (Access Time: 18.12.2020, 23:00)

- [47]<https://www.nursingtimes.net/> (Access Time: 18.12.2020, 23:04)
- [48]Tisdall, M., 2009. Non-invasive near infrared spectroscopy: a tool for measuring cerebral oxygenation and metabolism in patients with traumatic brain injury. MD Thesis. London: The Institute of Neurology University College London.
- [49]Tamura, Toshiyo, et al. (2014) "Wearable photoplethysmographic sensors past and present." *Electronics* 3.2 (2014): 282-302.
- [50]J. G. Webster, 1997, *Design of Pulse Oximeters*. IOP Publishing Ltd.
- [51]Elwell, C. & Hebden, J., 2000. Near-Infrared Spectroscopy. [Online] Available at: <http://medphys.ucl.ac.uk/research/> (Access Time: 18.12.2020, 23:00)
- [52]Mannheimer, P.D., 2007. The Light–Tissue Interaction of Pulse Oximetry. *Anesth Analg*, 105(6), pp.S10-17
- [53]Pulse Oximetry: Uses and Limitations, *The Journal for Nurse Practitioners*, Volume 3, Issue 5, 2007, Pages 312-317, ISSN 1555-4155,
- [54]Pulse oximetry: Understanding its basic principles facilitates appreciation of its limitations, Edward D. Chan, Michael M. Chan, Mallory M. Chan, *Respiratory Medicine*, Volume 107, Issue 6, 2013, Pages 789-799, ISSN 0954-6111

APPENDIX A

CIRCUIT SCHEMATIC



APPENDIX B

BILL OF MATERIALS

Element	Description	Designator	Footprint	LibRef	Quantity	Pricing (USD)
IC REG LINEAR 1.8V 600MA SOT25	Linear Voltage Regulator IC 1 Output 600mA SOT-25	1.8V LVR	AP2112K-1.8TRG1	AP2112K-1.8TRG1	1	0,47
IC REG LINEAR 3.3V 600MA SOT25	IC REG LINEAR 3.3V 600MA SOT25	3.3V LVR	AP2112K-3.3TRG1	AP2112K-3.3TRG1	1	0,47
CAP CER 10UF 16V X5R 0603	10µF, 16V, 0603	C1	Cap 10uF	CL10A106MO8NQNC	1	0,63
CAP CER 1UF 16V X5R 0603	1UF, 16V, 0603	C2, C3, C5, C6	Cap 1uF	CL10A105KO8NNNC	4	0,10
CAP CER 2.2UF 16V X5R 0603	2.2µF, 16V, 0603	C4	Cap 2.2uF	CL10A225KO8NNNC	1	0,10
IC SENSOR OXIMETER/HEARTRATE	Oximeter/Heart Rate Sensor I ² C Output	MAX30102	MAX30102	MAX30102EFD+	1	8,78
RES SMD 4.7K OHM 1% 1/8W 0603	RES SMD 4.7K OHM 1% 1/8W 0603	R1, R2, R3	Res 4.7K	MCT06030C4701FP500	3	0,16